



Inclusion complexation of 4',6-diamidino-2-phenylindole (DAPI) with cucurbit[7]uril and cyclodextrins (native β -, 2,6-di-O-methylated β -, and γ -cyclodextrin): characteristic inclusion behaviour and fluorescence enhancement

Yoshimi Sueishi¹ · Seiya Hagiwara¹ · Naoya Inazumi² · Tadashi Hanaya¹

Received: 24 August 2020 / Accepted: 22 December 2020 / Published online: 14 January 2021
© The Author(s), under exclusive licence to Springer Nature B.V. part of Springer Nature 2021

Abstract

Herein, we investigated the inclusion complexation of a fluorescent probe [4',6-diamidino-2-phenylindole (DAPI)] using various cyclodextrins (CDs) and cucurbit[7]uril (CB7). Using the continuous variation method, DAPI was found to form a 1:1 inclusion complex with CDs and CB7. ¹H-NMR and 2D ROESY (¹H-¹H rotating frame nuclear Overhauser effect) spectroscopy indicated that the inclusion of DAPI by the CDs and CB7 occurs via the encapsulation of the phenyl group and indole moiety of DAPI. The stability of the CB7 inclusion complex was higher than that of the CDs: the stability was attributed to the extra interaction formed between the dicationic dye (DAPI) and polar carbonyl groups at the portals of CB7. Furthermore, we determined the fluorescence quantum yield (Φ) of the inclusion complexes. The Φ values of DAPI were significantly enhanced upon its inclusion by CB7 and increased as the empirical solvent polarity parameter ($E_T(30)$) decreased. Based on these results, we concluded that the polarity of the microenvironment and protonation ability of the excited state of DAPI play important roles in emission efficiency.

Keywords DAPI · Cucurbit[7]uril · Cyclodextrin · Inclusion complexation · Enhancement of fluorescence

Introduction

4',6-Diamidino-2-phenylindole (DAPI) is a fluorescence probe for deoxyribonucleic acid (DNA) with important applications in compounds, such as antiparasitic, antibiotic, and anti-cancer drugs [1]. The fluorescence probe DAPI binds to DNA to form a stable complex in the minor groove of the A-T sequence [2] and is widely used in cell analysis to determine DNA content [3]. In many cases, fluorophores such as DAPI show high fluorescence emission efficiency

but are strongly quenched in polar solvents, such as water. DAPI has been employed as a polarity probe in various heterogeneous systems (for example, proteins) and host–guest inclusion complexes [2, 4]. Therefore, we believe that it is important to characterise the photochemical processes of DAPI.

The properties of fluorophores can be modulated using non-covalent host–guest interactions. β - and γ -Cyclodextrin (β - and γ -CD) are cyclic molecules consisting of seven and eight D-(+)-glucopyranose units, respectively, which possess hydrophobic cavities capable of forming inclusion complexes with organic molecules in an aqueous solution [5]. Cucurbit[7]uril (CB7) is another cage molecule, which has a pumpkin-shaped hydrophobic cavity with polar carbonyl groups at its portals. Thus, CB7 has received considerable attention as a versatile host molecule, and extensive studies have been reported on the inclusion complexation of DAPI with cyclodextrins (CDs) and CB7 [4, 6–9]. Miskolczyk et al. reported that DAPI produces a remarkably stable 1:1 inclusion complex with CB7 and discussed the fluorescence decay kinetics of DAPI [6]. In the inclusion of DAPI by

Supplementary Information The online version of this article (<https://doi.org/10.1007/s10847-020-01042-6>) contains supplementary material, which is available to authorized users.

✉ Yoshimi Sueishi
ysueishi@okayama-u.ac.jp

¹ Department of Chemistry, Faculty of Science, Okayama University, 3-1-1 Tsushima-naka, Kita-ku, Okayama 700-8530, Japan

² Technical Support Division, Graduate School of Science, Osaka University, Toyonaka, Osaka 560-0043, Japan

CDs, Shaikh et al. discussed the inclusion behaviour and photophysical properties of DAPI using absorption and time-resolved fluorescence measurements [7]. They suggested that the formation of inclusion complexes with CB7 and CDs retarded the excited-state protonation process for DAPI and enhanced fluorescence intensities. However, in the inclusion of CB7 and CDs, the inclusion behaviour and the effects of inclusion on the quantum yields of DAPI have not yet been sufficiently established.

Quantum yield (Φ) values are highly informative for characterising the photochemical processes exhibited by DAPI. In this study, we used a quantum efficiency analysis system equipped with a half-moon unit to determine accurate Φ values. The inclusion complexation of DAPI with three kinds of CDs (native β -CD, 2,6-di-*O*-methylated β -CD (DM- β -CD), and γ -CD) and CB7 was examined and the Φ values of their inclusion complexes were determined. We found that the fluorescent Φ values of DAPI were characteristically enhanced upon its inclusion with the CDs and CB7 studied. Based on our results, the inclusion behaviour of DAPI and its usefulness as a fluorescence probe have been discussed in detail.

Experimental

Materials

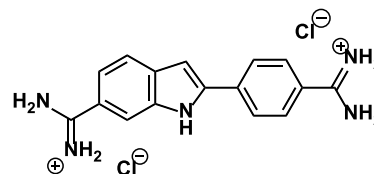
The structures of the guest (DAPI) and host (CDs and CB7) molecules are shown in Fig. 1.

The fluorescence probe DAPI (a specially prepared reagent) and the three kinds of CDs were purchased from Nacalai Tesque (Kyoto, Japan) and used without further purification. The water-soluble CB7 host was prepared according to the method reported by Marquez et al. [10] and recrystallised from acetone–water (purity > 97%). Water was purified by distillation and used as the solvent.

Fluorescence and NMR spectroscopy

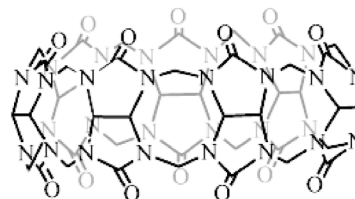
The fluorescence spectra of the DAPI complexes with CB7 and the CDs in water were recorded on a Shimadzu RF-5300PC spectrometer at an excitation wavelength of 361 nm at pH 7. The solution temperature was maintained using an external circulating water bath (± 0.2 K). The Φ values for DAPI were determined using an Otsuka Electronics Quantum Efficiency Analysis System (QE1000) equipped with a half-moon unit (Otsuka, Japan) at 298.0 ± 0.3 K. The Φ values were calibrated using quinine bisulfate solution in sulfuric acid (0.05 M (= mol dm⁻³)) as a standard; excitation wavelength = 347.5 nm and $\Phi = 0.51 \pm 0.02$ [11].

Guest molecule

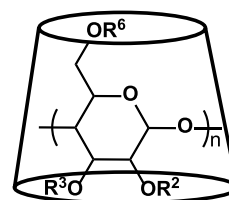


4',6-Diamidino-2-phenylindole (DAPI)

Host molecule



Cucurbit[7]uril (CB7)



Cyclodextrin (CD)

β -Cyclodextrin (β -CD ($n = 7$)): $R^2, R^3, R^6 = H$
 Heptakis(2,6-di-*O*-methyl)- β -cyclodextrin
 (DM- β -CD ($n = 7$)): $R^2, R^6 = CH_3, R^3 = H$
 γ -Cyclodextrin (γ -CD ($n = 8$)): $R^2, R^3, R^6 = H$

Fig. 1 The structures of guest and host molecules. Guest: DAPI. Host: three kinds of CDs and CB7

The ¹H NMR spectra of the inclusion complexes formed between DAPI and CB7 were recorded in D₂O using a Varian 400-MR ASW spectrometer (400 MHz) at 298 K. Chemical shifts (δ) are reported in ppm relative to HOD (δ 4.79) used as an internal standard. 2D ROESY-NMR measurements for the inclusion complexes of DAPI with the CDs were carried out with a Varian VNS 600 spectrometer (600 MHz). The mixing time for each ROESY-NMR measurement was 200 ms.

Results and discussion

Complexation of DAPI within the CDs and CB7

Upon addition of the CDs and CB7, a large increase in the fluorescence intensity in the vicinity of 460 nm was observed for DAPI. The typical fluorescence spectra of DAPI in the presence of β -CD and CB7 are shown in Fig. 1 and S1 (see Supplementary Information). Similar results were obtained for the complexation of DAPI with DM- β -CD and γ -CD. In order to confirm the stoichiometry of the complexation of DAPI with the CDs and CB7, fluorescence measurements were conducted by varying the molar fraction of DAPI and the host molecules, that is, a continuous variation method (Job's method) [12]. Job's plots for the changes in the fluorescence intensity of DAPI at various temperatures showed a maximum at a $[DAPI]/([DAPI] + [host])$ ratio of 0.5 (Figs. 1b and S2, see Supplementary Information), suggesting that the complexes formed between DAPI and the host molecules (CDs and CB7) exhibit 1:1 stoichiometry.

The equilibrium for the 1:1 complexation of DAPI (G) with the host molecules (H: CDs and CB7) can be expressed as follows:



where G@H denotes the guest–host inclusion complex. Under the conditions of $[H] \gg [G]$, the fluorescence spectra were analysed using the Benesi–Hildebrand (B–H) equation [13]:

$$\frac{[H]_0}{(F - F_0)} = \frac{1}{F - F_0} [H]_0 + \frac{1}{K[F - F_0]} \quad (2)$$

where $[H]_0$ denotes the initial concentration of the CDs and CB7, and F is the fluorescence intensity. F_∞ is the fluorescence intensity of DAPI complexed with the host molecules. Figure 2c shows that a good linear relationship was observed between $[H]_0/(F - F_0)$ and $[H]_0$; the complexation constants (K) for DAPI with the CDs were determined from the slope and intercept using Eq. 2. The results obtained at various temperatures are listed in Tables 1 and S1 (see Supplementary Information) and the dependence of temperature on the K values is shown in Fig. S3 in the Supplementary Information.

An analysis of the spectroscopic data using the B–H equation was not suitable for the inclusion complexation of DAPI with CB7 because of the extremely large K values. The Lang optimisation method was used to determine the complexation constants of CB7 [14].

$$\frac{[H]_0[G]_0}{F - F_0} = \left([H]_0 + [G]_0 - \frac{F - F_0}{F - F_0} \right) \frac{1}{F - F_0} + \frac{1}{(F - F_0)K} \quad (3)$$

The tentative values of $(F_\infty - F_0)$ and K obtained for the inclusion of DAPI within CB7 were estimated using Eq. 3 and a plot of $[H]_0[G]_0/(F - F_0)$ vs. $\{[H]_0 + [G]_0 - (F - F_0)/(F_\infty - F_0)\}$ was constructed using these values, producing new values from the linear relationship of Eq. 3. This procedure was repeated until the variation in the magnitude of the slope of the new plot using Eq. 3 converged to within 5%. Figure S1 (see Supplementary Information) shows the plots obtained using Eq. 3 and the K values observed for the CB7 inclusion complexes are listed in Table 1 and S1 (see Supplementary Information). Although the K values observed for CDs are somewhat large compared with those ($K_{\beta\text{-CD}} = 130 \text{ dm}^3 \text{ mol}^{-1}$ for β -CD) reported by Shaikh et al. [7], our observations are reasonable. The K values in Table 1 increase in the order of $\gamma\text{-CD} < \text{DM-}\beta\text{-CD} < \beta\text{-CD} < \text{CB7}$. In DM- β -CD, the methylation of the OH groups on the rim of the CD lengthens the cavity and enhances the inclusion ability via hydrophobic interactions. However, in the inclusion of DAPI, the K value for native β -CD was larger than those observed for DM- β -CD and γ -CD. Furthermore, although the binding constant observed for the complexation of DAPI with CB7 was slightly smaller than that ($K_{\text{CB7}} = 1.1 \times 10^7 \text{ dm}^3 \text{ mol}^{-1}$) reported by Miskolczy et al. [6], the K value observed for CB7 was found to be much larger than those for the CDs, suggesting that DAPI forms a more stable complex with CB7, which is responsible for the characteristic interaction observed between dicationic DAPI and the host molecule. The dicationic structure of DAPI at pH7 is also suggested by the $\text{p}K_a$ value (11.65 [15]) of DAPI.

To obtain useful information on the structure of the DAPI inclusion complexes, we conducted NMR measurements on the DAPI inclusion complexes with the CDs and CB7. Figures 3, S4, and S5 (Supplementary Information) show the ^1H - and 2D ROESY-NMR spectra of the DAPI inclusion complexes with the CDs. Figures 3a, b show that downfield shifts of the DAPI protons and large upfield shifts of the H(3,5) protons of DM- β -CD were observed with the addition of DAPI to the CD solution, indicating the encapsulation of DAPI into the DM- β -CD cavity. Furthermore, the relative intensities of the cross peaks of 2D ROESY-NMR measurements for the inclusion complexes are listed in Table S2 (Supplementary Information). In the inclusion of DM- β -CD (Fig. 3c), the cross peaks arising from the inner H(3,5) proton of DM- β -CD and H(2',6') protons of DAPI were observed, and the interactions of H(3',5') and H(4) protons of DAPI with the inner H(3) and H(5) protons of DM- β -CD were also detected, respectively, suggesting that the indole moiety of DAPI is

Fig. 2 **a** Fluorescence spectra obtained for DAPI ($2.49 \times 10^{-6} \text{ mol dm}^{-3}$) in an aqueous solution at 298 K: $[\beta\text{-CD}] = (0, (1) 0.50, (2) 1.00, (3) 1.50, (4) 3.00, (5) 4.99,$ and (6) $7.49 \times 10^{-3} \text{ mol dm}^{-3}$ (excitation at 361 nm). **b** Job's plots derived from the fluorescence data obtained for the inclusion complexation of DAPI with $\beta\text{-CD}$. **c** Determination of the inclusion equilibrium constant at 298 K: $[\text{DAPI}]_0 = 2.49 \times 10^{-6} \text{ mol dm}^{-3}$ and $[\beta\text{-CD}]_0 = 0.50 - 7.49 \times 10^{-4} \text{ mol dm}^{-3}$

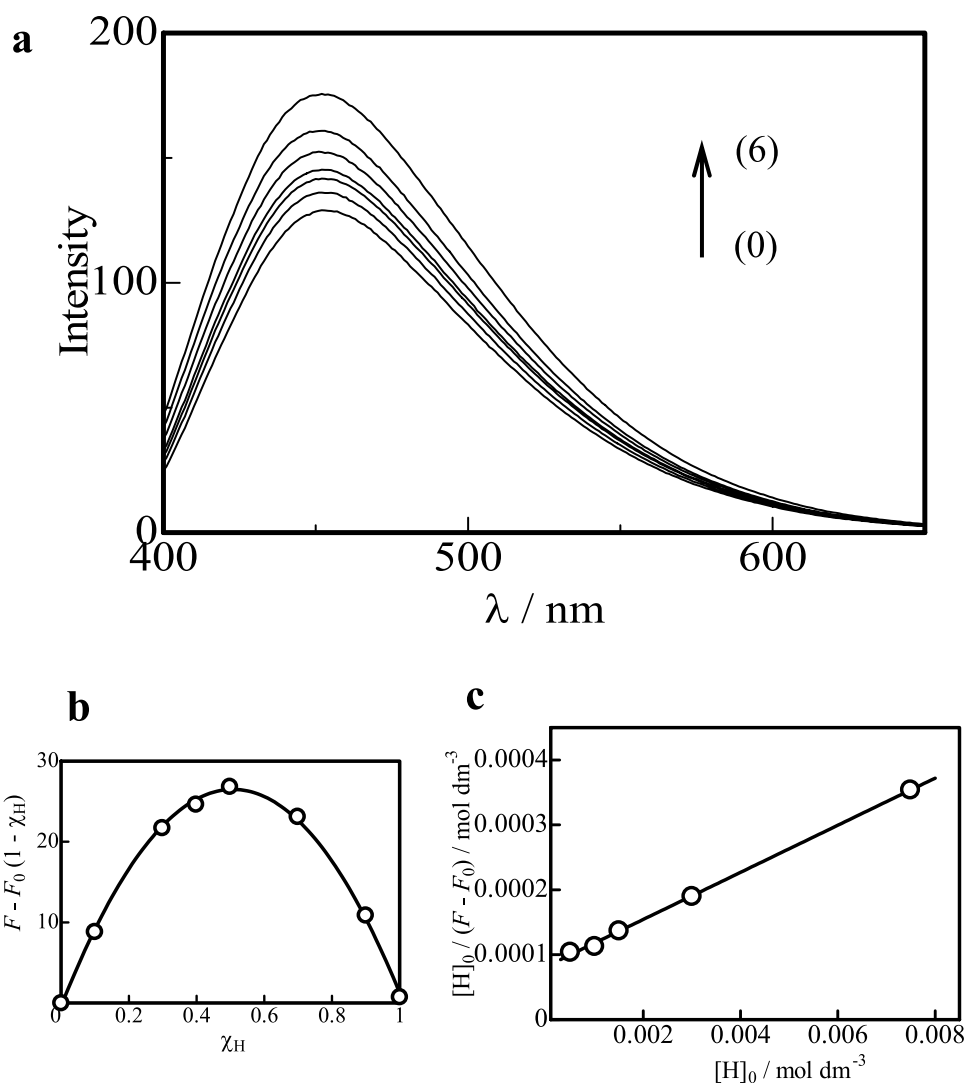


Table 1 Inclusion complexation constants and thermodynamic parameters for the inclusion complexation of DAPI with the CDs and CB7 in water

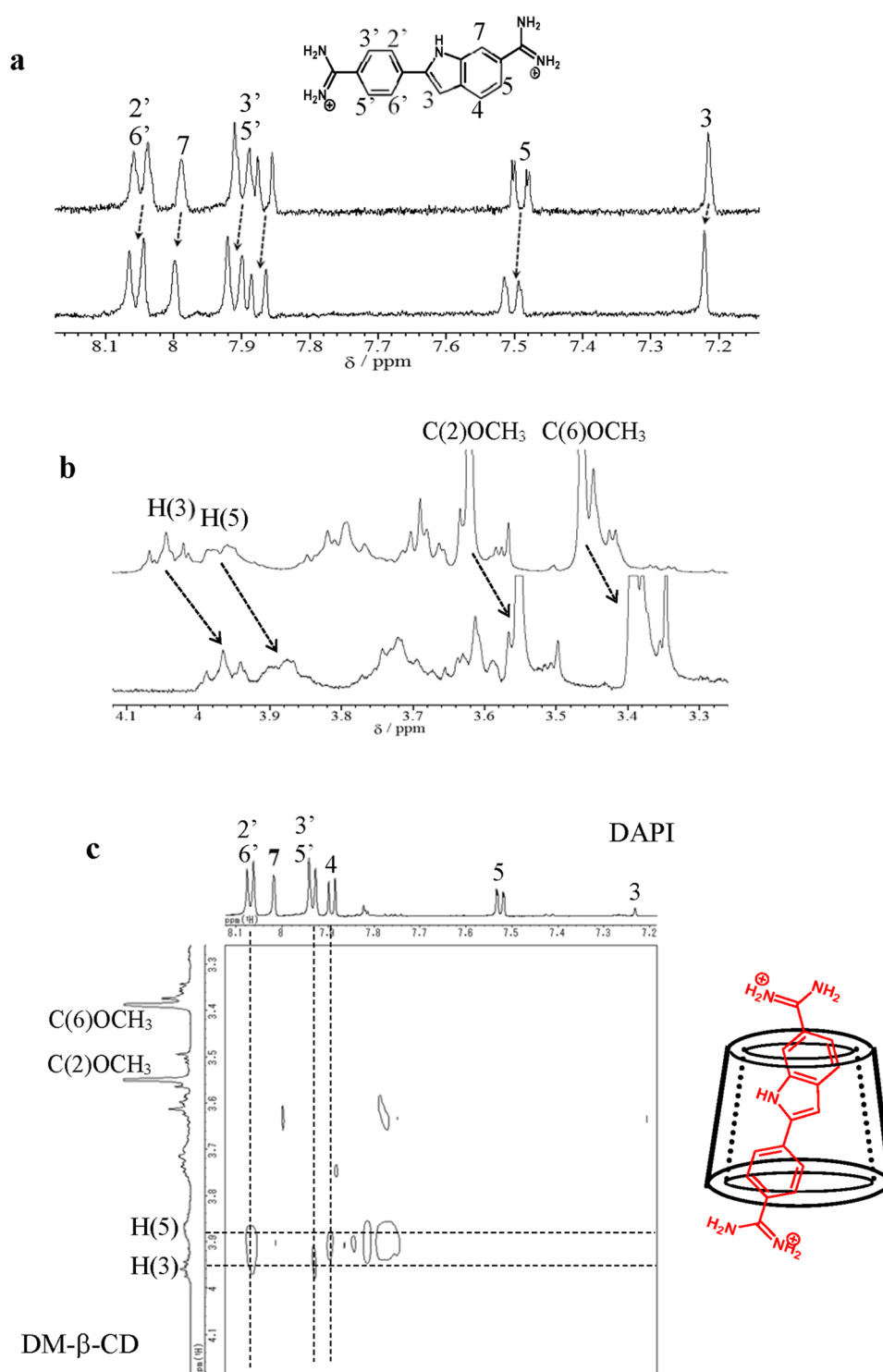
Host	$10^{-3} K$ (at 298 K) ($\text{dm}^3 \text{ mol}^{-1}$)	ΔH° (kJ mol^{-1})	ΔS° ($\text{J K}^{-1} \text{ mol}^{-1}$)	$\Delta G^\circ_{298 \text{ K}}$ (kJ mol^{-1})
CB7	3030 ± 16	-11.5 ± 0.3	85.4 ± 0.9	-36.9 ± 0.9
$\beta\text{-CD}$	0.435 ± 0.006	55.6 ± 2.3	237 ± 8	-15.0 ± 3.3
DM- $\beta\text{-CD}$	0.274 ± 0.002	81.3 ± 2.3	319 ± 8	-13.8 ± 3.3
$\gamma\text{-CD}$	0.130 ± 0.003	61.7 ± 2.8	248 ± 9	-12.6 ± 3.9

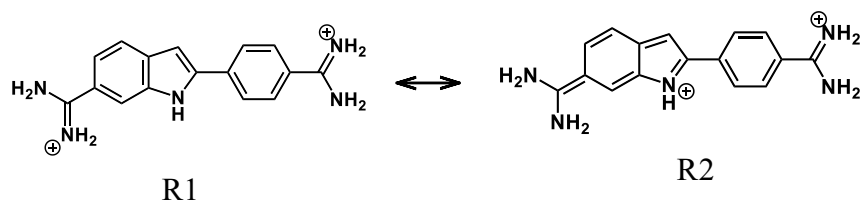
placed at the narrow end of DM- $\beta\text{-CD}$ (a reversed orientation when compared to that observed for the native $\beta\text{-CD}$ inclusion complex) and that the phenyl group and indole moiety are included in the DM- $\beta\text{-CD}$ cavity. The results for β - and γ -CDs can be summarised as follows: (1) During the inclusion of DAPI within $\beta\text{-CD}$, the phenyl group and indole moiety of DAPI are encapsulated inside the cavity,

and the phenyl group is located at the narrow end of $\beta\text{-CD}$. (2) During the inclusion of DAPI within $\gamma\text{-CD}$, the phenyl group and indole moiety of DAPI are encapsulated at the wide end of $\gamma\text{-CD}$. Plausible structures for the inclusion complexes formed between DAPI and the CDs are shown in Figs. 3, S4, and S5 (see Supplementary Information).

Figure S6 (Supplementary Information) shows the ^1H NMR spectra recorded for the inclusion complex formed between DAPI and CB7. The NMR shifts induced by the inclusion of DAPI in CB7 indicate that the phenyl group of DAPI is located in the CB7 cavity, and that the indole moiety and $-\text{NH}_2$ substituent of the phenyl group are located close to the polar carbonyl groups at the portals of CB7. As depicted in the DAPI resonance form, the $-\text{N}(\delta^+)\text{H}$ (indole nitrogen) and $-\text{N}(\delta^+)\text{H}_2$ substituents on the phenyl group are reasonably located close to the polar carbonyl groups of the portals in the inclusion complex, suggesting that the contribution from resonance structure R2 is reinforced by inclusion in CB7.

Fig. 3 ^1H NMR (**a** DAPI and **b** DM- β -CD) and 2D ROESY-NMR spectra (**c** the DAPI inclusion complex) for the DAPI complexation with DM- β -CD in D_2O : **a** $[\text{DAPI}]_0 = 1.81 \times 10^{-3} \text{ mol dm}^{-3}$ and $[\text{DM-}\beta\text{-CD}]_0 =$ (upper) 0 and (lower) $3.19 \times 10^{-3} \text{ mol dm}^{-3}$, **b** (upper) $[\text{DM-}\beta\text{-CD}]_0 = 2.39 \times 10^{-3} \text{ mol dm}^{-3}$; (lower) $[\text{DAPI}]_0 = 1.81 \times 10^{-3} \text{ mol dm}^{-3}$ and $[\text{DM-}\beta\text{-CD}]_0 = 3.19 \times 10^{-3}$, and **c** $[\text{DAPI}]_0 = 1.81 \times 10^{-3} \text{ mol dm}^{-3}$ and $[\text{DM-}\beta\text{-CD}]_0 = 3.19 \times 10^{-3} \text{ mol dm}^{-3}$





Thermodynamic parameters obtained for the complexation of DAPI with CDs and CB7

The K values obtained for the complexation of DAPI with CDs and CB7 at various temperatures are listed in Table S1 (see Supplementary Information). The K values for the CD inclusion increase with increasing temperature. Conversely, in the CB7 inclusion, the K values decrease with temperature. The inclusion behaviour can be understood by the changes in the enthalpy and entropy (ΔH° and ΔS°) observed during the inclusion process. The ΔH° and ΔS° values of the CDs and CB7 were determined from the slope and intercept of their corresponding van't Hoff plots using the complexation constants (Fig. S3 in Supplementary Information); the results are listed in Table 1.

The ΔG° values, which express the stability of the inclusion complexes, are listed on the right of Table 1. In the inclusion complexation of CDs, the $-\Delta G^\circ$ values are attributed to the increase in the contact area of the hydrophobic body of the guest molecule in the CD cavity [5]. The $-\Delta G^\circ$ value for DM- β -CD is smaller than that of native β -CD, which is responsible for the dicationic property of DAPI. The $-\Delta G^\circ$ value for the CB7 inclusion is remarkably larger than those of CDs. We believe that in the CB7 inclusion, the extra interaction by the polar CB7 rim is operative. In the inclusion complexation of DAPI with CDs, large and positive ΔS° values (driving force of inclusion) were obtained and are responsible for the loss of freedom observed upon the association and desolvation of dicationic DAPI [16]. The negative ΔH° value observed for the DAPI@CB7 complexation indicates that an inclusion complex is formed in which the van der Waals interactions are dominant due to the tight fit of DAPI within the CB7 cavity.

A linear relationship between ΔH° and ΔS° values was obtained for the complexation of DAPI within the CDs (Fig. 4), suggesting that a single mechanism was in operation during the complexation process [17]. During the inclusion of DAPI within CB7, a large downward shift from this linear relationship was observed. This shift for CB7 was

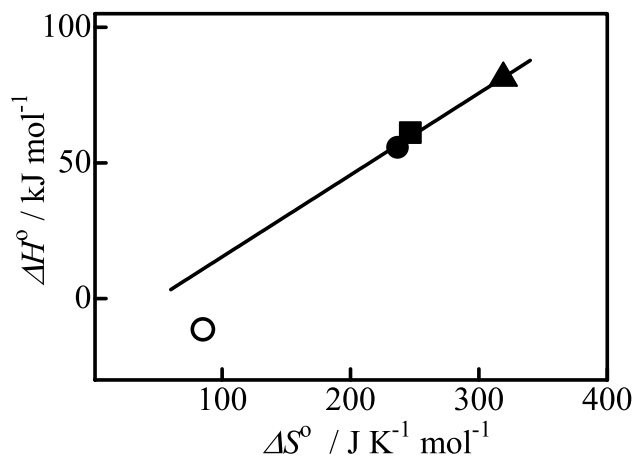


Fig. 4 ΔH° – ΔS° relationship for the inclusion equilibrium of DAPI within the CDs and CB7: Filled circle: β -CD, filled triangle: DM- β -CD, filled square: γ -CD, and circle: CB7

Table 2 Quantum yields (Φ_{complex})^a obtained for the inclusion complexes of DAPI with the CDs and CB7 in water and local polarity values ($E_T(30)_{\text{app}}$) of DAPI within the cavity of the CDs and CB7

Host	Φ_{complex}	$\Phi_{\text{complex}}/\Phi_{\text{guest}}$	$E_T(30)_{\text{app}}$ (kJ mol ⁻¹)
–	0.0381 ± 0.0004	1	–
CB7	0.226 ± 0.006	5.93	244.0
β -CD	0.0461 ± 0.0007	1.21	263.0
DM- β -CD	0.0712 ± 0.0023	1.86	259.1
γ -CD	0.0503 ± 0.0012	1.32	261.7

^aAt 298 K and pH 7

not attributed to a mechanism change, but to an extra free-energy change from the stabilisation of the complex formed between DAPI and CB7, as explained above.

Fluorescence quantum yields of the inclusion complexes

The quantum yield (Φ) values obtained for the inclusion complexes are highly informative for understanding the inclusion behaviour and fluorescence processes observed for DAPI. The Φ values obtained for the inclusion complexes were determined using fluorescence spectroscopy and determined using the following equation [18]:

$$\phi = \frac{FP_{\text{complex}}}{AP_{\text{complex}}} = \frac{FP - FP_{\text{guest}}}{AP - AP_{\text{guest}}} \quad (4)$$

where FP_{complex} , FP_{guest} , and FP denote the fluorescence photon numbers of the inclusion complex, free guest, and apparent solution, respectively. Similarly, AP denotes the excitation photon number. The concentration of the free guest (DAPI) was evaluated using the complexation constants and the obtained Φ values are listed in Table 2. Inclusion by the CDs slightly enhanced the Φ values, and it is noteworthy that the Φ value of DAPI was strongly enhanced by its inclusion within CB7.

Anilinoanthracene sulfonic acid (ANS) is sensitive to the polarity of its local environment and represents a useful fluorescence probe [16]. To discuss its usefulness as a fluorescence probe, we examined the fluorescence emission maxima and Φ values obtained for DAPI in different dioxane–water mixtures. Figure 4 shows the plots of the Φ values observed for DAPI against the empirical solvent polarity parameters ($E_T(30)$ value) in different dioxane–water solutions. Figure 4 and Table S3 (see Supplementary Information) show that although the Φ values of DAPI obtained in the dioxane–water mixtures increase as the $E_T(30)$ value decreases, the DAPI emission maxima are not sensitive to the polarity of the solvent, suggesting that the fluorescence quenching process of DAPI was different from that of ANS, in which the rate of the non-radiative process from the intramolecular charge transfer state increases in a polar solvent [19].

Regarding the DAPI fluorescence process, Miskolczy et al. reported that binding to CB7 prevents protonation of the indole moiety in the excited-state and the formation of two conformers with distinct properties in the ground state [6]. Shaikh et al. suggested that DAPI in aqueous solution primarily exists as a planar conformer and in the inclusion complexes of DAPI with CDs, the access of solvent water molecules to the indole nitrogen is significantly reduced, resulting in the retardation of the excited-state protonation in the CD inclusion complex of DAPI compared with free DAPI [7]. Szabo et al. reported that the indole ring of the planar configuration becomes much basic in the excited-state and rapid proton transfer from the 6-amidinium group to the indole ring occurs [20]. Furthermore, they suggested that on

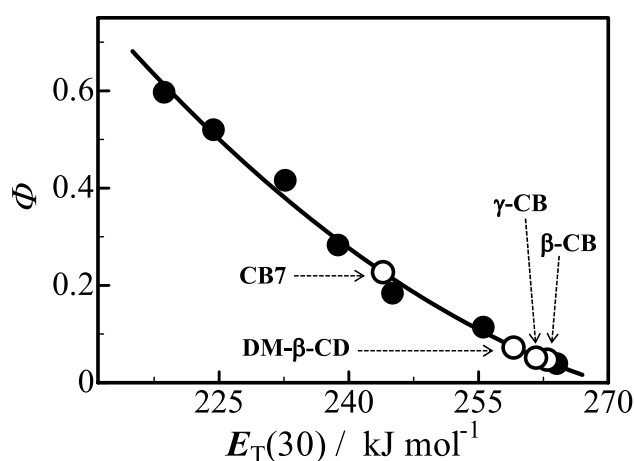


Fig. 5 Plot of the Φ values obtained for DAPI and its inclusion complexes versus the empirical polarity parameter $E_T(30)$ value

binding DAPI to nucleic acids, the loss of the rapid intramolecular proton transfer in the excited-state to the indole ring is responsible for the fluorescence enhancement. The inclusion complex formation by CDs and CB7 largely retards the solvent-mediated excited-state protonation process for DAPI and enhances its fluorescence quantum yields. A large enhancement was observed for the Φ value of DAPI during its inclusion within CB7. As expected from the contribution of the DAPI resonance structure, the acidity of the indole nitrogen in the ground state of DAPI decreases inside the CB7 cavity, leading to significant retardation of the solvent-mediated excited-state protonation.

The decrease in Φ values observed with increasing solvent polarity (Fig. 5) also supports the notation that the local polarity and protonation ability of the DAPI excited-state are important factors for the fluorescence process. Figure 5 shows that the local polarity of the DAPI excited-state inside the cavities of the CDs and CB7 can be tentatively evaluated as $E_T(30)$ (kJ mol^{-1}) = 259–263 (CDs) and 244 (CB7) using the Φ values obtained for the inclusion complexes formed by DAPI (Table 2). The determination of the Φ values for the inclusion complexes of DAPI within the CDs and CB7 provides useful information for the local polarity and solvent-mediated protonation ability at indole nitrogen (steric hindrance), resembling the process of substrate binding to the enzymes.

In summary, the complexation constants and fluorescence Φ values for the inclusion complexes formed between DAPI and various CDs and CB7 were determined. Based on the NMR spectra of the inclusion complexes, the characteristic disposition of DAPI within the cavities of the CDs and CB7 was confirmed. The inclusion complex formed between DAPI and CB7 showed a significantly enhanced Φ value, which can be explained by the fluorescence quenching mechanism of DAPI. Furthermore, the Φ value of DAPI

was sensitive to solvent polarity. We suggest that the local polarity and protonation ability of the indole nitrogen atom play important roles in Φ value enhancement. We believe that we were able to show the usefulness of the Φ values obtained for the functional fluorophore DAPI.

References

- Baraldi, P.G., Bovero, A., Fruttarolo, F., Preti, D., Tabrizi, M.A., Pavani, M.G., Romagnoli, R.: DNA minor groove binders as potential antitumor and antimicrobial agents. *Med. Res. Rev.* **24**, 475–528 (2004)
- Tanius, F.A., Veal, J.M., Buczak, H., Ratmeyer, L.S., Wilson, W.D.: DAPI(4',6-diamidino-2-phenylindole) binds differently to DNA and RNA: minor-groove binding at AT sites and intercalation at AU sites. *Biochemistry* **31**, 3103–3112 (1992)
- Kapuscinski, J.: DAPI: a DNA-specific fluorescent probe. *Biotech. Histochem.* **70**, 220–233 (1995)
- Frankewich, R.P., Thimmaiah, K.N., Hinze, W.L.: Evaluation of the relative effectiveness of different water-soluble β -cyclodextrin media to function as fluorescence enhancement agents. *Anal. Chem.* **63**, 2924–2933 (1991)
- Saenger, W.: Cyclodextrin inclusion compounds in research and industry. *Angew. Chem. Int. Ed. Engl.* **19**, 344–362 (1980)
- Miskolczy, Z., Biczok, L., Megyesi, M., Jablonkai, I.: Inclusion complex formation of Ionic liquids and other cationic organic compounds with cucurbit[7]uril studied by 4',6-diamidino-2-phenylindole fluorescent probe. *J. Phys. Chem. B* **113**, 1645–1651 (2009)
- Shaikh, M., Mohanty, J., Bhasikuttan, A.C., Pal, H.: Host-guest interaction of 4',6-diamidino-2-phenylindole (DAPI) with β and γ cyclodextrins: modulation in the photophysical properties. *J. Spectrosc. Dyn.* **2**, 1–14 (2012)
- Douza, N., Pischel, U., Nau, W.M.: Fluorescent dyes and their supramolecular host/guest complexes with macrocycles in aqueous solution. *Chem. Rev.* **111**, 7941–7980 (2011)
- Shinde, M.N., Bhasikuttan, A.C., Mohanty, J.: The contrasting recognition behavior of β -cyclodextrin and its sulfobutylether derivative towards 4',6-diamidino-2-phenylindole. *ChemPhysChem* **16**, 3425–3432 (2015)
- Marquez, C., Huang, F., Nau, W.M.: Cucurbiturils: molecular nanocapsules for time-resolved fluorescence-based assays. *IEEE Trans. Nanobiosci.* **3**, 39–45 (2004)
- Velapoldi, R.A., Tonnesen, H.H.: Corrected emission spectra and quantum yields for a series of fluorescent compounds in the visible spectra region. *J. Fluorescence* **14**, 465–472 (2004)
- Job, P.: Formation and stability of inorganic complexes in solution. *Ann. Chim.* **9**, 113–203 (1928)
- Scott, R.L.: Some comments on the Benesi-Hildebrand equation. *Recueil des Travaux Chimiques des Pays-Bas et de la Belgique* **75**, 787–789 (1956)
- Lang, R.P.: Molecular complexes and their spectra. XIV. Iodine complexes with thiourea and thioacetamide. *J. Am. Chem. Soc.* **84**, 1185–1192 (1962)
- Yasujima, T., Ohta, K., Inoue, Ishimaru, M.K., Yuasa, H.: Evaluation of 4',6-diamidino-2-phenylindole as a fluorescent probe substrate for rapid assays of the functionality of human multidrug and toxin extrusion proteins. *Drug. Metab. Dispos.* **38**, 715–721 (2011)
- Castronuovo, G., Niccoli, M., Varriale, L.: Complexation forces in aqueous solution. Calorimetric studies of the association of 2-hydroxypropyl- β -cyclodextrin with monocarboxylic acids or cycloalkanols. *Tetrahedron* **63**, 7047–7052 (2007)
- Leffler, J.E.: The interpretation of enthalpy and entropy data. *J. Org. Chem.* **31**, 533–537 (1966)
- Sueishi, Y., Matsumoto, Y., Kimata, Y., Osawa, Y., Inazumi, N., Hanaya, T.: Characterization of group-inclusion complexations of rhodamine derivatives with native and 2,6-di-O-methylated β -cyclodextrins. *J. Incl. Phenom. Macrocycl. Chem.* **96**, 365–372 (2020)
- Kosower, E.M., Dodiuk, H.: Intramolecular donor-acceptor systems. 3. A third type of emitting singlet state for N-alkyl-6-N-arylamino-2-naphthalenesulfonates. Solvent modulation of substituent effects on charge-transfer emissions. *J. Am. Chem. Soc.* **100**, 4173–4179 (1978)
- Szabo, A.G., Krajcarski, D.T., Cavatorta, P., Masott, L., Barcellona, M.L.: Excited state pKa behaviour of DAPI. A rationalization of the fluorescence enhancement of DAPI in DAPI-nucleic acid complexes. *Photochem. Photobiol.* **44**, 143–150 (1986)

Publisher's Note Springer Nature remains neutral with regard to jurisdictional claims in published maps and institutional affiliations.